Journal of Solid State Chemistry **153,** 82–91 (2000)
doi:10.1006/jssc.2000.8750, available online at http://www.idealibrary.com on IDEAL®

Anomalous Spin Crossover of Mechanically Strained Iron(II) Complexes with 1,10-Phenanthroline with Their Counterions, NCS^- and PF_6^-

Naoko Tsuchiya, Atsushi Tsukamoto, Tadashi Ohshita, Tetsuhiko Isobe, Mamoru Senna,[1] Naoki Yoshioka, and Hidenari Inoue

Department of Applied Chemistry, Faculty of Science and Technology, Keio University, 3-14-1, Hiyoshi, Yokohama, 223–8522, Japan

Received February 1, 2000; in revised form April 11, 2000; accepted April 20, 2000; published online July 7, 2000

Effects of counterions on the change in the magnetic behavior due to mechanical amorphization have been examined on iron(II) complexes with 1,10-phenanthroline, $Fe(phen)_2(NCS)_2$, $[Fe(phen)_3](NCS)_2 \cdot H_2O$, and $[Fe(phen)_3](PF_6)_2$, at temperatures between 2 K and 300 K. Amorphization results in the increase in $\chi_M T$, where χ_M is molar magnetic susceptibility and T is temperature, in two modes, i.e., a jump at temperatures below 20 K and a subsequent gradual increase. The first mode is attributed to the mechanically induced high spin state ($^5T_{2g}$) which is made metastable below 20 K. The second is the thermally induced transition from a low spin ($^1A_{1g}$) to a high spin ($^5T_{2g}$) state for the distorted complexes with the widened distribution of the ligand field strength. The stabilization of the HS state is mainly due to the ligand field distortion caused by mechanical amorphization. Coordination of ionic species, NCS^- and PF_6^-, originally serving as counterions, plays a significant role in the ligand field distortion. © 2000 Academic Press

Key Words: **iron(II) complex crystals; spin crossover; mechanical stressing; counterion; ligand field strength.**

INTRODUCTION

Strained crystals show various anomalies in physicochemical and electronic properties. One of the general reasons is the change in the electronic states and related transition probability due to loss of the symmetry in crystal and ligand fields. This is particularly significant for transition metals in view of various magnetic or optical properties. Partial allowance of the forbidden d–d transition of Mn^{2+} incorporated in ZnS, for instance, enhances photoluminescence intensity (1).

An energy level of octahedrally symmetrical 3d electrons in Fe^{2+} in a complex compound is split into two states, e_g and t_{2g}, with a finite separation, Δ_0 (2–5). The separation depends on the strength of crystal field. As a consequence, the $3d^6$ configuration of the complex takes two different spin states, i.e., a low spin (LS) state ($^1A_{1g}$) described as $(t_{2g})^6(e_g)^0$, and a high spin (HS) one ($^5T_{2g}$), $(t_{2g})^4(e_g)^2$.

The crystal field stabilization energy (CFSE) is defined as $2.4\Delta_0 - 3P$ for the LS state and $0.4\Delta_0 - P$ for the HS state, where P is an electron pairing energy (4). Since the energy difference between LS and HS states is $2(\Delta_0 - P)$, the LS state is more stable under the condition, $\Delta_0 > P$. When the energy difference, $2(\Delta_0 - P)$, is surmounted by thermal energy, k_BT, spin transition from LS to HS occurs, where k_B is the Boltzmann constant. The elongation of the Fe^{2+}–ligand bond accompanies the spin transition. This is attributed to the presence of two electrons within the e_g (d_{z^2} and $d_{x^2-y^2}$) orbitals which lie along the Fe^{2+}–ligand donor atom vector and have the stronger repulsion than t_{2g} (d_{xy}, d_{yz}, and d_{zx}) orbitals (4, 6).

The spin transition behavior, i.e., Δ_0, depends not only on the difference of ligands, intraligand substitutuents (5–7), and counteranions (5, 8, 9), but also on the environmental conditions. When a complex is intercalated in an interplanar space of layered material, its effective magnetic moment, μ_{eff}, jumps up at lower temperatures (10, 11). Nakano *et al.* also observed a similar spin crossover for $[Fe(amp)_3]^{2+}$ (amp = 2-(aminomethyl)pyridine) intercalated in montmorillonite (11). They consistently attribute the spin transition to the stabilization of the HS state by the reduction of the energy difference between the HS ($^5T_{2g}$) and LS ($^1A_{1g}$) states.

Likewise, Tiwary *et al.* reported that $[Co(bpy)_3]^{2+}$ (bpy = 2, 2′-bipyridine) encapsulated in zeolite-Y has a near-octahedral geometry and exhibits a spin crossover phenomenon, although the trigonally distorted $[Co(bpy)_3]^{2+}$ retains the HS state ($^4T_{1g}$) both in solution and in the solid state (12, 13). According to the calculation of the angular orbital ligand field model, the energy difference between the LS (^2E_g) and HS ($^4T_{1g}$) states increases by

[1]To whom correspondence should be addressed.
Fax: + 81-45-564-0950. E-mail: senna@applc.keio.ac.jp.

0022-4596/00 $35.00

encapsulation to allow a thermally induced spin transition (13). Thus, we may generalize that the spin state is determined by the molecular geometry of a coordination complex, such as the metal (M)–ligand (L) distance, the L–M–L angle, and the symmetry of coordination. The geometrical configuration of individual complexes and three-dimensional arrangement of complexes depend mutually on each other.

We have observed two different modes of spin transition, i.e., jumps and a gradual increase in mechanically amorphized $[Fe(phen)_3](NCS)_2 \cdot H_2O$ (14). Crystalline $[Fe(phen)_3](NCS)_2 \cdot H_2O$ exhibits a diamagnetic LS state at least below 330 K. In contrast, amorphous $[Fe(phen)_3](NCS)_2 \cdot H_2O$ shows peculiar magnetic behavior; i.e., μ_{eff} or $\chi_M T$ ($\propto \mu_{eff}{}^2$, where χ_M is the molar magnetic susceptibility and T is temperature) jumps twice at around 20 K and 190 K. The latter jump is close to the spin transition temperature for $Fe(phen)_2(NCS)_2$ (5, 15). Since the magnetic behavior of the milled complex is very similar to those of the intercalated, distorted complexes (10, 11), it is reasonable to assume that the ligand field strength is reduced by the distortion of coordination bonds as a consequence of milling. The mode of $\chi_M T$ change with temperature differs markedly among similar complexes with different counterions, i.e., $Fe(phen)_2(NCS)_2$, $[Fe(phen)_3](NCS)_2 \cdot H_2O$, and $[Fe(phen)_3](PF_6)_2$. Therefore, we focus in this study on the role of counterions on the anomalous spin crossover of the mechanically strained complex compounds.

EXPERIMENTAL

Synthesis

The preparation method for $[Fe(phen)_3](NCS)_2 \cdot H_2O$ was given in Ref. (14). Calculated values for $C_{38}H_{26}FeN_8OS_2$ are C, 62.5%; H, 3.6%; N, 15.3%. Analytical results are C, 63.8%; H, 3.1%; N, 15.6%. As-purchased $[Fe(phen)_3](PF_6)_2$ (Aldrich, No. 38, 831-9; calculated values for $C_{36}H_{24}F_{12}FeN_6P_2$ are C, 48.7%; H, 2.7%; N, 9.5%; Fe, 6.3%; analytical results are C, 43.0%; H, 2.2%; N, 8.3%; Fe, 5.4%.) was used. $Fe(phen)_2(NCS)_2$ was synthesized in the manner reported by Ganguli *et al.* (16). A methanol solution of iron(II) sulfate heptahydrate was prepared by dissolving 1.11 g (4 mmol) of $FeSO_4 \cdot 7H_2O$ (Kanto, purity $> 99.0\%$) in 30 cm^3 of methanol, containing 10 mg of L-ascorbic acid (Kishida, purity $> 99.5\%$). A 30 cm^3 methanol solution of 0.78 g (8 mmol) of potassium thiocyanate (Yoneyama, purity $> 99.5\%$) was added dropwise to this solution. After the solution was stirred for 1 h, the precipitate was filtered off. A 30 cm^3 methanol solution of 1.59 g (8 mmol) of 1,10-phenantroline monohydrate (Yoneyama, purity $> 99.0\%$) was added dropwise to the filtrate containing Fe^{2+} and NCS^- with stirring. After 3 h, the pink-violet precipitate of $Fe(phen)_2(NCS)_2$ was filtered, washed with methanol, and dried at 0.1 Pa and room temperature for 24 h. All operations were carried out under an argon atmosphere. Calculated values for $C_{26}H_{16}F_{12}FeN_6S_2$ are C, 58.6%; H, 3.0%; N, 15.8%. Analytical results are C, 58.2%; H, 2.9%; N, 15.7%.

Mechanical Treatment

External stress was applied by milling with a planetary ball-mill (originally supplied from URF as AGO II and modified by Nara Machinery). A sample (0.5 g) was put into a 27 cm^3 Al_2O_3-lined vial together with sixteen 10-mm yttrium-stabilized zirconia balls. The gas inside the vial was replaced by Ar and the vial was sealed before milling. Milling time was fixed at 5 h. Details of the planetary ball-mill are given elsewhere (17).

Characterization

The crystalline structures were examined by X-ray diffractometry (XRD) (Rigaku, Rint2000). Far-infrared (far-IR) absorption spectra (Bio-Rad, FTS40V) under 0.1 Pa were measured in the range 500–150 cm^{-1} at a resolution of 2 cm^{-1} to analyze coordination bonds. Samples were dispersed in polyethylene pellets in far-IR measurements.

Changes in the electronic states of Fe^{2+} and ligands were examined by UV-vis diffuse reflectance spectroscopy (JASCO, V–550) and ^{57}Fe Mössbauer spectroscopy. UV–vis spectra were measured between 800 nm and 200 nm at a scan speed of 100 nm $\cdot$ min^{-1} and at intervals of 0.5 nm. An MgO plate was used as a reflection standard. Mössbauer spectra were obtained with a 370 MBq ^{57}Co source in Rh foil (the Radiochemical Centre, Amarsham). The velocity scale was calibrated using the absorption peaks of an iron film. The curve fitting was carried out by using a least-squares procedure assuming that the observed peak shape is Lorentzian. All the measurements were carried out at room temperature.

The temperature dependence of the magnetic properties was measured by using a superconducting quantum interference device (SQUID) magnetometer (Quantum Design, MPMS5) at 500 mT when the temperature was increased from 2 K to 300 K.

RESULTS

Temperature Dependence of $\chi_M T$

The product of molar magnetic susceptibility, χ_M, and temperature, T, is plotted as a function of temperature in Fig. 1. The intact complex, $Fe(phen)_2(NCS)_2$, exhibits a typical spin crossover around 190 K, as shown by triangles in Fig. 1a. After milling of the sample for 5 h, we observe two marked increases in the $\chi_M T$ for $Fe(phen)_2(NCS)_2$, as shown by circles in Fig. 1a. The height of the low-temperature jump of $\chi_M T$ increases by 4 times after milling, followed by a

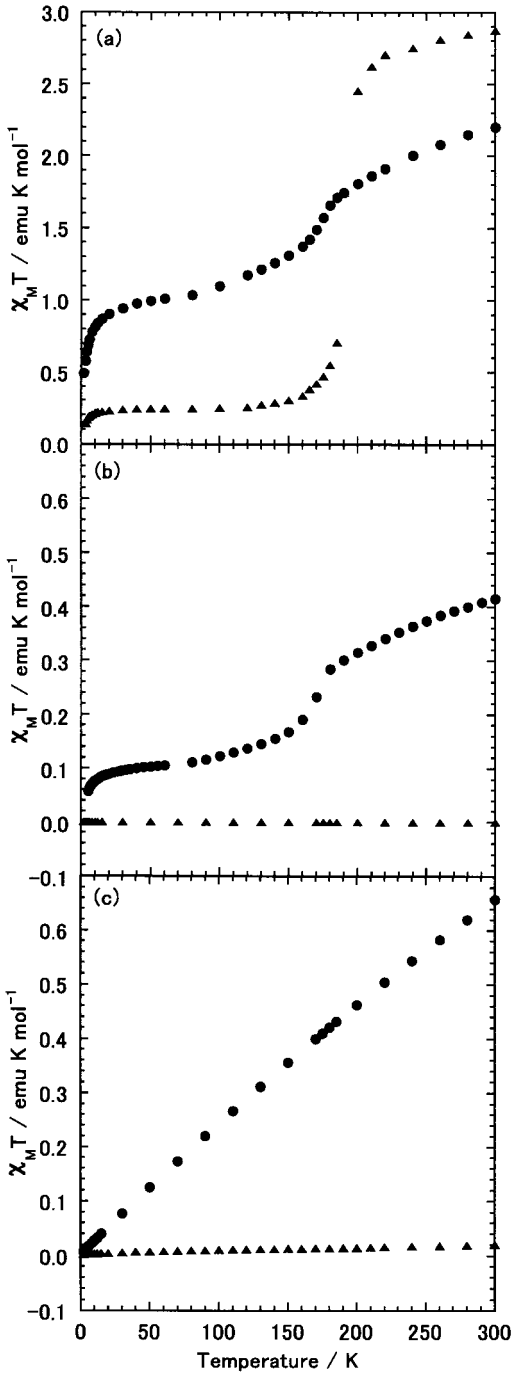

FIG. 1. Temperature dependence of $\chi_M T$ for (a) $Fe(phen)_2(NCS)_2$, ▲, intact; ●, after milling for 5 h; (b) $[Fe(phen)_3](NCS)_2.H_2O$, ▲, intact; ●, after milling for 5 h; and (c) $[Fe(phen)_3](PF_6)_2$, ▲, intact; ●, after milling for 5 h.

gradual increase. The HS state might remain at temperatures below 20 K, since this jump of $\chi_M T$ is due to magnetic interaction among complexes with HS states and/or zero-field splitting of the spin quintet state (6). A usual spin crossover around 190 K decreases to a significant extent with a slight decrease in the onset temperature.

The intact complexes, $[Fe(phen)_3](NCS)_2 \cdot H_2O$ and $[Fe(phen)_3](PF_6)_2$, exhibit diamagnetism, as shown by triangles in Figs. 1b and 1c, respectively. The shape of the curve, shown by circles in Fig. 1b for $[Fe(phen)_3](NCS)_2 \cdot H_2O$ after milling for 5 h, is very close to that of $Fe(phen)_2(NCS)_2$, although the entire change is one-fifth of the latter. In a sharp contrast to the complexes containing NCS^-, the value of $\chi_M T$ for $[Fe(phen)_3](PF_6)_2$ after milling for 5 h increases quasi-linearly without any sharp increase, as shown in Fig. 1c.

Changes in Crystallinity and Coordination Bonds by Milling

The XRD patterns of the samples of $Fe(phen)_2(NCS)_2$ and $[Fe(phen)_3](PF_6)_2$ with and without milling are shown in Fig. 2. Similar to the observation for $[Fe(phen)_3](NCS)_2 \cdot H_2O$ in our previous report (14), the complex crystals amorphize after milling. Thus, counterions do not affect the mechanical amorphization, as far as the long-range ordering detectable by XRD is concerned.

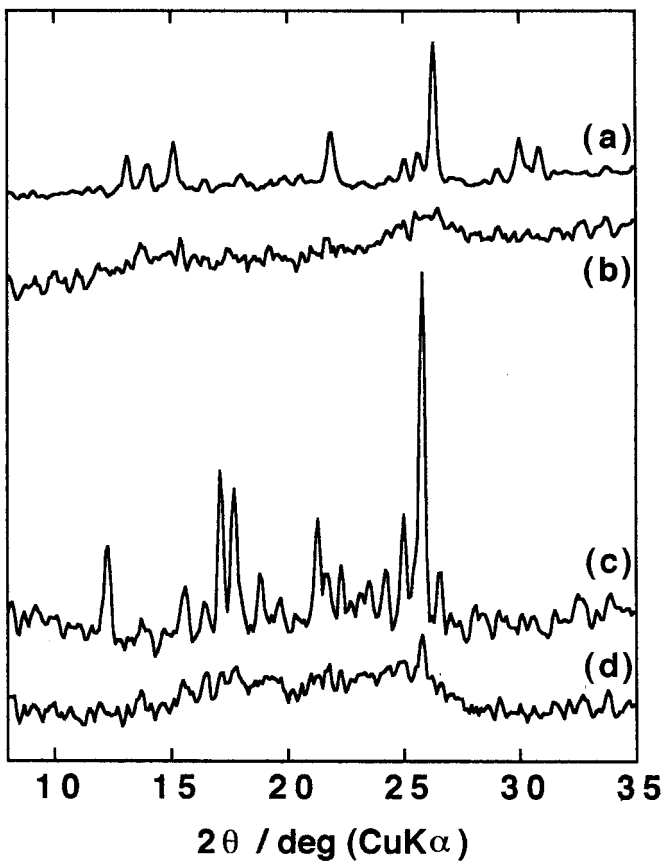

FIG. 2. XRD profiles of $Fe(phen)_2(NCS)_2$ (a) intact and (b) after milling for 5 h, and $[Fe(phen)_3](PF_6)_2$ (c) intact and (d) after milling for 5 h.

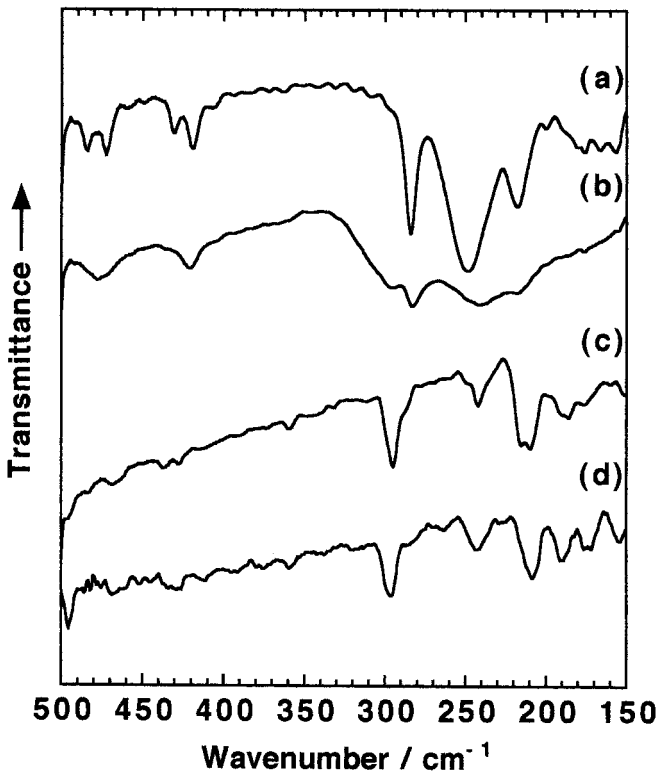

FIG. 3. Far-IR spectra of $Fe(phen)_2(NCS)_2$ (a) intact and (b) after milling for 5 h, and $[Fe(phen)_3](PF_6)_2$ (c) intact and (d) after milling for 5 h.

Curves (a) and (b) in Fig. 3 show far-IR absorption spectra of $Fe(phen)_2(NCS)_2$ before and after milling, respectively. The absorption bands at 249 cm^{-1} and 218 cm^{-1} are the stretching vibrations of Fe–N (NCS) and Fe–N (phen) in complexes with the HS states, respectively (18–21). The intact $Fe(phen)_2(NCS)_2$ shows the doublet bands at 419 cm^{-1} and 431 cm^{-1} due to the out-of-plane phen ring deformation (22), and at 473 cm^{-1} and 484 cm^{-1} due to coordinated NCS bending vibration (15, 22). The band splittings disappear after milling. The IR band at 284 cm^{-1} is assigned to the ligand vibration activated by complex formation (20). All the absorption peaks become broader after milling. These tendencies are similar to those found for $[Fe(phen)_3](NCS)_2 \cdot H_2O$ in our previous report (14). Note that a new peak appears at 296 cm^{-1} after milling. This peak is close to those of phen vibration, observed in the LS state of $Fe(phen)_2(NCS)_2$ at 100 K (21).

The intact $[Fe(phen)_3](PF_6)_2$ shows IR bands at 209 cm^{-1} and 217 cm^{-1} due to the deformation vibration of N(phen)–Fe–N(phen) (Figs. 3c and 3d) (23–25). The IR band at 209 cm^{-1} does not shift toward lower wavenumbers, while the IR band at 217 cm^{-1} disappears after milling. The changes in the IR spectrum of $[Fe(phen)_3](PF_6)_2$ are smaller than those of $Fe(phen)_2(NCS)_2$ and $[Fe(phen)_3](NCS)_2 \cdot H_2O$.

Ligand Fields around Iron(II)

Mössbauer spectra are shown in Figs. 4a–4f and their parameters are listed in Table 1. Two doublet peaks from the HS and LS states are observed in both spectra of $Fe(phen)_2(NCS)_2$ without and with milling (Figs. 4a, 4b, and 5). Although the peak area proportion of the LS state in the intact $Fe(phen)_2(NCS)_2$ is 34%, the amount of LS states must be less than 34% because of the larger recoil-free fraction of LS state. By milling, the peak widths, Γ, for LS state increase by a factor of 1.5. The peak area fraction of the LS state increases from 34% to 64% upon milling.

The intact $[Fe(phen)_3](NCS)_2 \cdot H_2O$ (Fig. 4c) is in the LS state, judging from the values of the isomer shift, δ, and the quadropole splitting, ΔE_Q, 0.31 mm s^{-1} and 0.26 mm s^{-1}, respectively (26). After milling, a new doublet peak with $\delta = 1.06$ mm s^{-1} and $\Delta E_Q = 2.39$ mm s^{-1} appears (Fig. 4d). These new peaks are assigned to the HS state (5). At the

TABLE 1
Parameters of Mössbauer Spectra at Room Temperature

		Fig.	δ/mm s^{-1}	ΔE_Q/mm s^{-1}	Γ/mm s^{-1}	Spain state
$Fe(phen)_2(NCS)_2$	intact	4a	0.97	2.61	0.31	HS(66%)[a]
			0.23	0.33	0.35	LS(34%)
	milled	4b	0.97	2.57	0.31	HS(36%)
	for 5 h		0.28	0.28	0.52	LS(64%)
$[Fe(phen)_3(NCS)_2 . H_2O$	intact	4c	0.31	0.26	0.26	LS
	milled	4d	1.06	2.39	0.24	HS(9%)
	for 5 h		0.28	0.24	0.35	LS(91%)
$[Fe(phen)_3(PF_6)_2$	intact	4e	0.32	0.28	0.26	LS
	milled	4f	0.25	0.40	0.36	LS(49%)
	for 5 h		0.28	—	0.34	LS(51%)

[a]The peak area fraction.

same time, the value of Γ for the LS state increases by a factor of 1.3. The doublet peak with $\delta = 0.32\ \mathrm{mm\,s^{-1}}$ and $\Delta E_Q = 0.28\ \mathrm{mm\,s^{-1}}$ is observed in the spectrum of the intact $[Fe(phen)_3](PF_6)_2$ (Fig. 4e) and it is also assigned to the LS state. After milling, the parameter Γ increases by a factor of 1.4 (Fig. 4f). A new single peak with $\delta = 0.28\ \mathrm{mm\,s^{-1}}$ appears and is assigned to the LS state (26). The doublet peak due to the HS state is not observed even after milling.

Electronic States

Figure 5(a) shows UV–vis spectra of $Fe(phen)_2(NCS)_2$ with their assignments (Table 2). The intact sample exhibits bands at 255 nm and 298 nm due to the $\pi^* \leftarrow \pi$ transition and a band at 544 nm due to metal-to-ligand charge transfer (MLCT) (15). The intensity of the MLCT band relative to the largest $\pi^* \leftarrow \pi$ band, *a*, increases by 49% after milling.

The MLCT broad band at $\sim$460 nm and the $\pi^* \leftarrow \pi$ bands at around 250 nm are observed in the spectrum of the intact $[Fe(phen)_3](NCS)_2 \cdot H_2O$, as shown by a broken line in Fig. 5b, where the assignments are based on those for $[Fe(phen)_3]^{2+}$ ions dissolved in the solvent (27). The value of *a* increases by 23% after milling, as shown by a solid line in Fig. 5b. It is noteworthy that not only the value of *a* but also the shape of the UV–vis spectrum of the milled

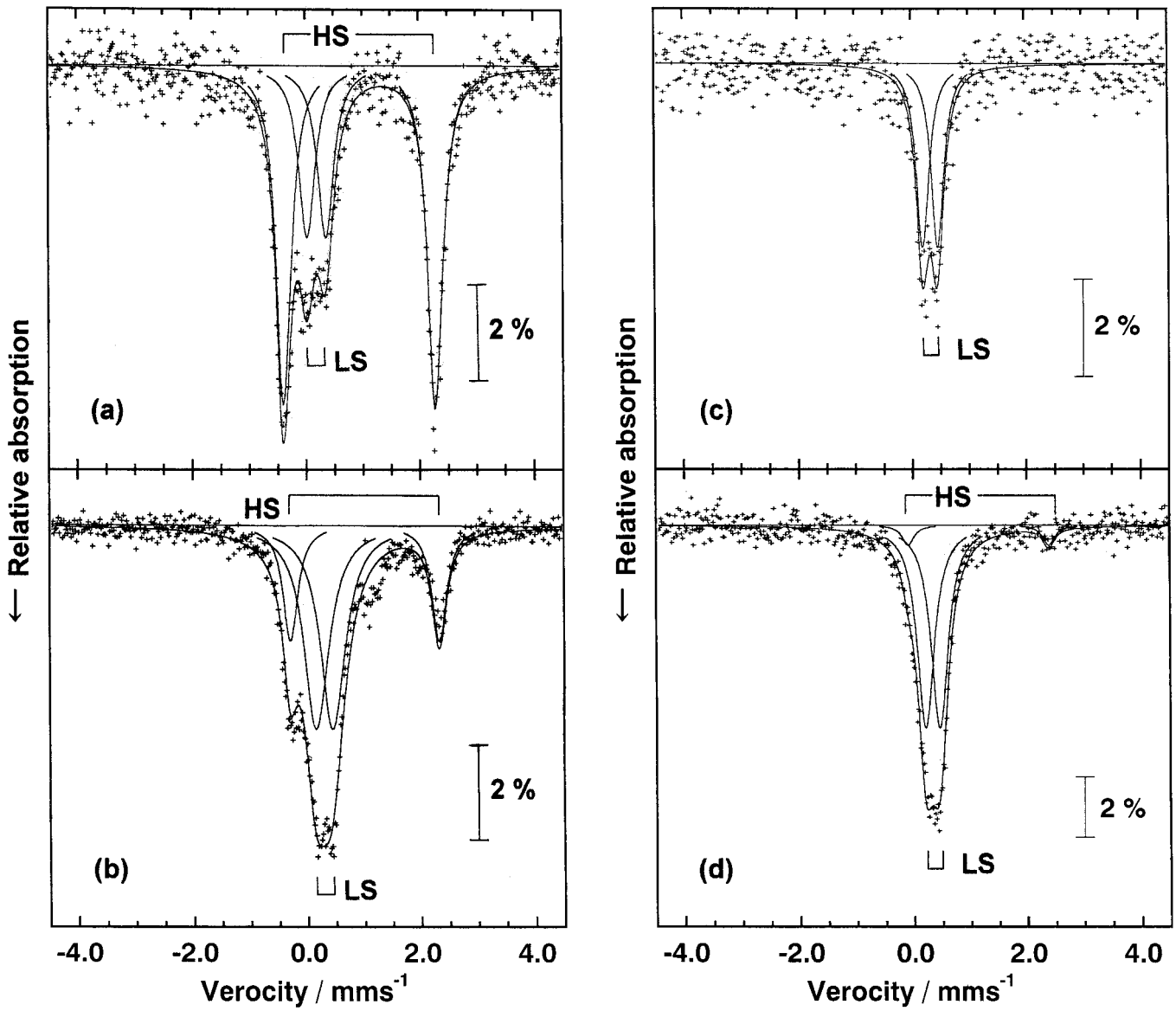

FIG. 4. Mössbauer spectra of $Fe(phen)_2(NCS)_2$ (a) intact and (b) after milling for 5 h; $[Fe(phen)_3](NCS)_2 \cdot H_2O$ (c) intact and (d) after milling for 5 h, and $[Fe(phen)_3](PF_6)_2$, (e) intact and (f) after milling for 5 h.

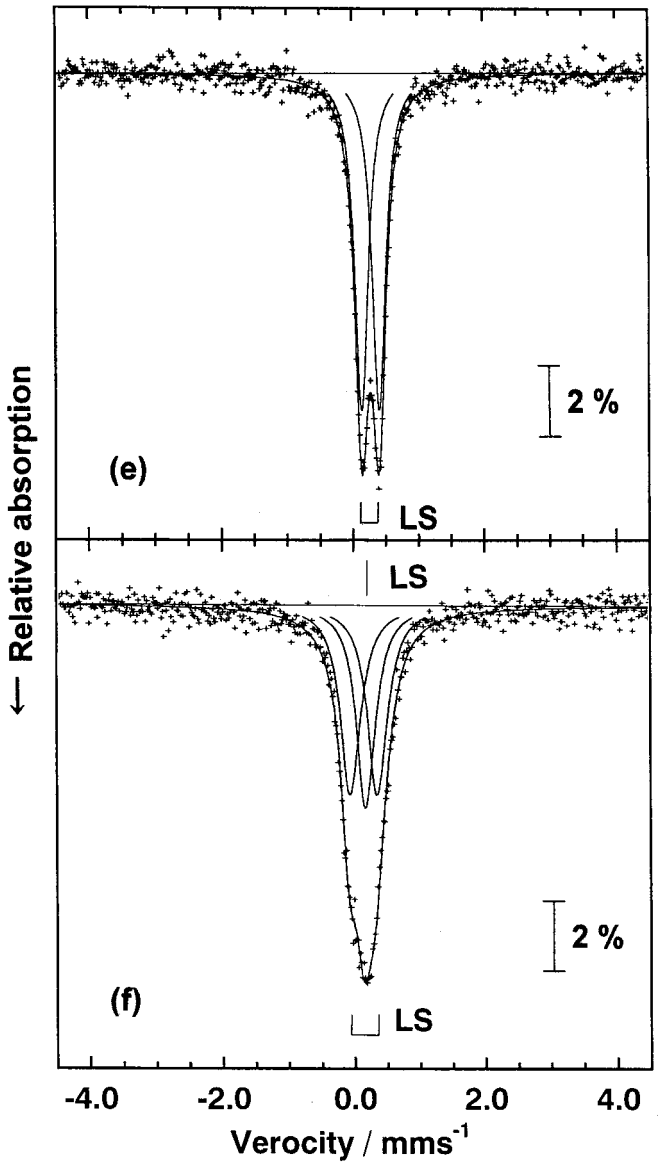

FIG. 4—*Continued*

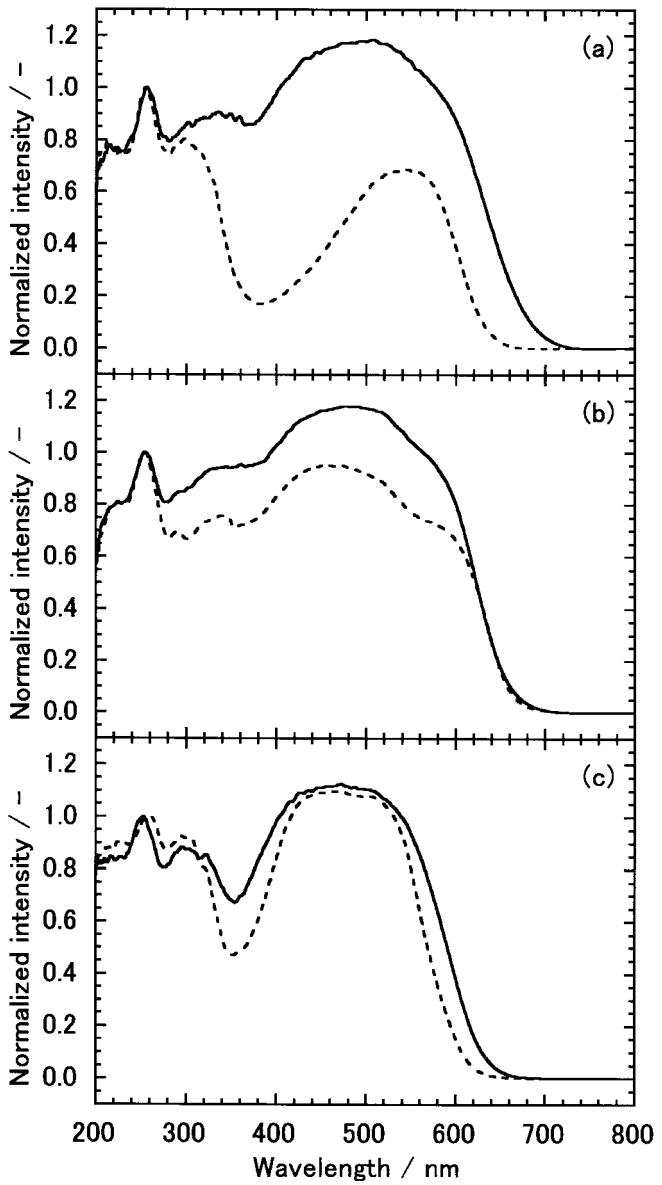

FIG. 5. UV–vis spectra for (a) $Fe(phen)_2(NCS)_2$, ---, intact and —, after milling for 5 h; (b) $[Fe(phen)_3](NCS)_2 \cdot H_2O$, ---, intact and —, after milling for 5 h; and (c) $[Fe(phen)_3](PF_6)_2$, ---, intact and —, after milling for 5 h. The vertical axis is normalized so that top of the peak of the largest $\pi^* \leftarrow \pi$ band is unity, in order to evaluate the peak ratio, *a*.

$[Fe(phen)_3](NCS)_2 \cdot H_2O$ are similar to those of the milled $Fe(phen)_2(NCS)_2$.

The MLCT band at 472 nm and the $\pi^* \leftarrow \pi$ bands at 260 nm and 294 nm are observed in the intact $[Fe(phen)_3](PF_6)_2$ (Fig. 5c). The value of *a* increases by only 2% after milling, in contrast to the cases of $Fe(phen)_2(NCS)_2$ and $[Fe(phen)_3](NCS)_2 \cdot H_2O$. Thus, the change in the UV–vis spectrum of $[Fe(phen)_3](PF_6)_2$ upon milling is much smaller than those of $[Fe(phen)_3](NCS)_2 \cdot H_2O$ and $Fe(phen)_2(NCS)_2$.

DISCUSSION

Change in the Coordination State

An increase in $\chi_M T$ due to milling was always observed. However, a distinct difference among the complexes is observed in the mode of the increase, particularly at temperatures below 20 K. While a jump in $\chi_M T$ appeared in $Fe(phen)_2(NCS)_2$ and $[Fe(phen)_3](NCS)_2 \cdot H_2O$, the value of $\chi_M T$ increased only gradually in $[Fe(phen)_3](PF_6)_2$. The difference in the mode is discussed below in the light of structure-related electronic states. Thermally induced spin crossover observed near 190 K for the milled sample of $[Fe(phen)_3](NCS)_2 \cdot H_2O$ is also to be elucidated.

Since no difference in the mechanical amorphization behavior was observed for the three iron(II) complexes, the

TABLE 2
Assignments and Peak Intensities of UV–Vis Spectra

Intact			Milled for 5 h				
Wavelength/nm	Intensity[a]/—	a^b/—	Wavelength/nm	Intensity/—	a/—	Assignment	Δa^c/—
			$Fe(phen)_2(NCS)_2$				
544	0.69	0.69	505	1.18	1.18	MLCT	+ 0.49
298	0.80		335	0.90		$\pi^* \leftarrow \pi$	
255	1.00		255	1.00		$\pi^* \leftarrow \pi$	
213	0.79		215	0.79		$\pi^* \leftarrow \pi$	
			$[Fe(phen)_3](NCS)_2 \cdot H_2O$				
459	0.95	0.95	472	1.18	1.18	MLCT	+ 0.23
338	0.75		339	0.94		$\pi^* \leftarrow \pi$	
254	1.00		254	1.00		$\pi^* \leftarrow \pi$	
222	0.81		222	0.80		$\pi^* \leftarrow \pi$	
			$[Fe(phen)_3](PF_6)_2$				
472	0.10	1.10	472	1.12	1.12	MLCT	+ 0.02
294	0.91		295	0.88		$\pi^* \leftarrow \pi$	
260	1.00		253	1.00		$\pi^* \leftarrow \pi$	
228	0.89		—	—		$\pi^* \leftarrow \pi$	

[a] Normalized intensity, evaluated by taking the peak top of the largest $\pi^* \leftarrow \pi$ band to be unity.
[b] Relative intensity of MLCT band to the largest $\pi^* \leftarrow \pi$ band.
[c] The difference in a between intact and milled samples.

arrangement of complexes, i.e., long-range ordering, cannot play a dominant role in the changes in the magnetic behavior described above. In contrast, the change in the coordination state, i.e., the short-range ordering, is specific to each complex in many aspects. Broadening of IR absorption bands assigned to phen ring deformation and Fe–N stretching vibration is always observed below 300 cm^{-1} after milling, particularly for $Fe(phen)_2(NCS)_2$. An increase in the distribution of the bond nature is suggested by this kind of broadening. The IR bands due to N(phen)–Fe–N(phen) deformation of $[Fe(phen)_3](NCS)_2 \cdot H_2O$ shift remarkably toward the lower wavenumbers as well. This indicates the weakening of the Fe–N bonds by milling of highly symmetric $[Fe(phen)_3](NCS)_2 \cdot H_2O$ (14).

The changes in the intramolecular bonding state of $[Fe(phen)_3](PF_6)_2$ are relatively small compared to those with NCS^- as a counterion. Thus, a loss of the symmetry in a complex to a greater extent under mechanical stress tends to exhibit a low-temperature jump in $\chi_M T$. This kind of change is found in the case of the complexes with NCS^- ions.

Change in the Electronic States

The octahedral symmetry of iron(II) complexes became lower upon milling. This is reflected in the large peak width, Γ, of the Mössbauer spectra due to the wider distribution of the electronic state of Fe^{2+} after milling. On top of that, we observed the new doublet peak due to the HS state after milling $[Fe(phen)_3](NCS)_2 \cdot H_2O$. The Mössbauer parameters, δ and ΔE_Q, of the HS state are close to those of $Fe(phen)_2(NCS)_2$. It is well known that $[Fe(phen)_3](NCS)_2 \cdot H_2O$ is diamagnetic as long as its intrinsic high symmetry is preserved. In our previous paper (14), we examined the C–N stretching vibration in IR spectra. The milled sample of $[Fe(phen)_3](NCS)_2 \cdot H_2O$ shows IR bands due to both free and coordinated NCS^-. A part of the ligand, phen, is therefore exchanged with NCS^- upon milling of a complex $[Fe(phen)_3](NCS)_2 \cdot H_2O$, resulting in the partial formation of $Fe(phen)_2(NCS)_2$. In contrast, no HS doublet was observed in the Mössbauer spectrum of milled $[Fe(phen)_3](PF_6)_2$. Judging from the $\chi_M T$ values of $[Fe(phen)_3](NCS)_2 \cdot H_2O$ and $[Fe(phen)_3](PF_6)_2$, HS components other than $Fe(phen)_2(NCS)_2$ are expected. The absence of the absorption peaks of the HS components in the Mössbauer spectra may be attributed to their small recoil-free fraction and/or too small relaxation time compared to the time scale of Mössbauer spectroscopy. In the case of too small relaxation time, analysis with the relaxation model could explain the peak broadenings and allow estimation of the other HS components (28, 29). The new single peak due to the LS state after milling $[Fe(phen)_3](PF_6)_2$ is also associated with the wider distribution of the electronic state of Fe^{2+} after milling.

The increase in the value a was observed for the UV–vis spectra of $Fe(phen)_2(NCS)_2$ and $[Fe(phen)_3](NCS)_2 \cdot H_2O$

after milling. The increase in the value a suggests broadening of the distribution of the ligand field strength to both the higher and lower wings.

The similarity of the UV–vis spectra between $Fe(phen)_2(NCS)_2$ and $[Fe(phen)_3](NCS)_2 \cdot H_2O$ also suggests an exchange between the ligand and the counterion, i.e., phen and NCS^-, by milling. As a result, a small amount of $Fe(phen)_2(NCS)_2$ is produced from $[Fe(phen)_3](NCS)_2 \cdot H_2O$. This accords well with the results of IR (14) and Mössbauer spectroscopy discussed above. In the case of $[Fe(phen)_3](PF_6)_2$, however, the increase in a is only 2%, being much smaller than those in the other complexes. Hence, the change in the ligand symmetry is correspondingly small. Thus, the coordination compound with NCS^- as a counterion exhibits a larger change in the coordination bonds under mechanical stress. This leads to a higher probability of the exchange reaction between the ligand and the counterion.

One of the most significant features in the milled samples, especially for $Fe(phen)_2(NCS)_2$ and $[Fe(phen)_3](NCS)_2 \cdot H_2O$, is the distribution of strain in Fe^{2+}–N coordination bonds and those of electronic states. As a consequence, ligand field symmetry is gradually lost as confirmed by IR, Mössbauer, and UV–vis spectra. Thus, mechanical treatment increases various kinds of heterogeneity. As the values of $\chi_M T$ suppress above 200 K in the milled $Fe(phen)_2(NCS)_2$, not only HS states are metastabilized below 20 K but also the fraction of LS states increases at temperatures between 2 K and 300 K.

Two Modes for Temperature Dependence of $\chi_M T$

An energy gap diagram between t_{2g} and e_g, i.e., the ligand field splitting parameter, Δ_0, for Fe^{2+} ($3d^6$) in O_h symmetry is given in Fig. 6a. After milling, the molecular symmetry deviates from O_h. The degree of deviation is not uniform, as mentioned above. However, the molecular strain after milling is represented by Δ_0 which serves as a measure of the deviation from O_h symmetry. The value Δ_0 is distributed between $\Delta_0 - \delta_1$ and $\Delta_0 + \delta_2$, (δ_1, $\delta_2 > 0$), as shown in Fig. 6b. A widened distribution of the ligand field strength upon milling is verified by a wider spectrum due to coordination bonds, as described above.

An energy level diagram for Fe^{2+} ($3d^6$) is given in Fig. 7. The value of Δ_0 for intact complexes, $[Fe(phen)_3](NCS)_2$ and $[Fe(phen)_3](PF_6)_2$, is larger than $\Delta_{0,tr}$, where the energy difference between the LS and HS states is zero on the ordinate, at temperatures below 300 K. Therefore, the ground state is LS state. For the milled complexes, thermally induced spin transition begins for the LS state with the smallest $\Delta_0 - \delta_1$ and propagates gradually to the states of larger Δ_0. This explains a gradual increase of $\chi_M T$ with increasing temperature for all the milled complexes. In addition, larger ligand field splitting, $\Delta_0 + \delta_2$, suppresses the

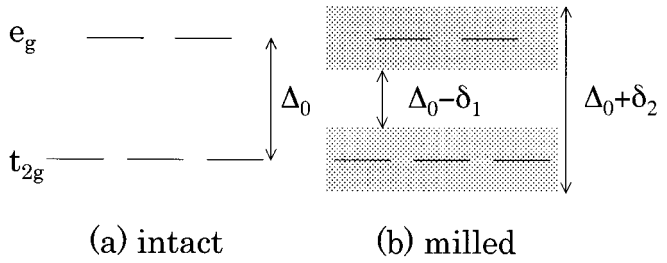

FIG. 6. Energy gap between t_{2g} and e_g, Δ_0, of $Fe^{2+}(3d^6)$ in (a) octahedral and (b) distorted environment.

transition from the LS to the HS states, as observed in Fig. 1a for $Fe(phen)_2(NCS)_2$ above 200 K.

If milling decreases the ligand field strength to $\Delta_0 - \delta_1$, less than $\Delta_{0,tr}$, a ground state changes from the LS to the HS states. Consequently, milling produces a metastable HS state. We propose such a transition as a "mechanically induced spin transition." The mechanically induced HS state might remain at temperatures below 20 K, showing the observed jump of $\chi_M T$ due to magnetic interaction among complexes with HS states and/or zero-field splitting of the the spin quintet state (6). This jump is observed for $Fe(phen)_2(NCS)_2$ and $[Fe(phen)_3](NCS)_2 \cdot H_2O$ after milling, but not for $[Fe(phen)_3](PF_6)_2$. The extent of the jump is 10 times larger for milled $Fe(phen)_2(NCS)_2$ than for milled $[Fe(phen)_3](NCS)_2 \cdot H_2O$. The latter contains a small amount of $Fe(phen)_2(NCS)_2$ formed by an exchange reaction between counterions and ligands, as mentioned above. Hence, the mechanically induced HS state is closely related to the distorted $Fe(phen)_2(NCS)_2$.

The increase of $\chi_M T$ for milled $[Fe(phen)_3](NCS)_2 \cdot H_2O$ at around 190 K is quite similar to that of $Fe(phen)_2(NCS)_2$ with and without milling. This is due to the partial exchange of phen with NCS^- which originally serves as a counterion

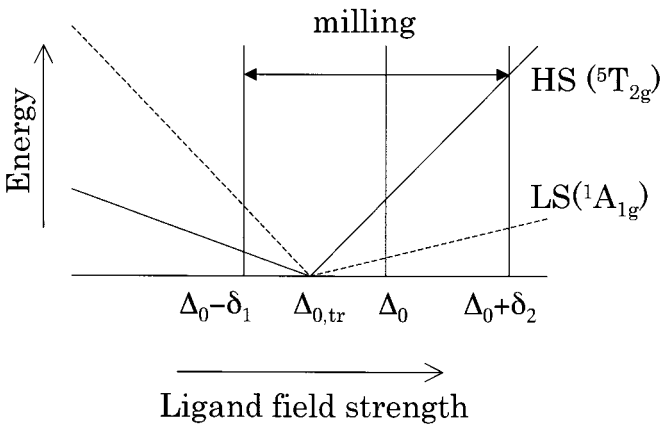

FIG. 7. Schematic energy level diagram of $Fe^{2+}(3d^6)$ as a function of the ligand field strength, Δ_0.

of $[Fe(phen)_3](NCS)_2 \cdot H_2O$. This partial ligand exchange is also confirmed by IR (14), Mössbauer, and UV–vis spectra. The formation of $Fe(phen)_2(NCS)_2$ from $[Fe(phen)_3](NCS)_2 \cdot H_2O$ decreases the symmetry of the ligand field around Fe^{2+}, and hence widens the distribution of Δ_0. This is consistent with the above-mentioned discussion.

Ligand Exchange and Flexibility of Complexes under Mechanical Stress

The ligand, phen, is partly replaced by NCS^- which was a counterion of $[Fe(phen)_3](NCS)_2 \cdot H_2O$ before milling. The absence of the jumping increase of $\chi_M T$ in $[Fe(phen)_3](PF_6)_2$ could, then, be explained by the smaller chance of the ligand exchange between phen and PF_6^-, as compared to the case of $[Fe(phen)_3](NCS)_2 \cdot H_2O$.

Coordination bonds in $Fe(phen)_2(NCS)_2$ and $[Fe(phen)_3](NCS)_2 \cdot H_2O$ are able to deform considerably, as discussed above. Complexes with three phen ligands are highly symmetrical and thus less deformable. The flexibility of $[Fe(phen)_3]^{2+}$ compounds depends, however, on the species of the counterion, as well. Since linear NCS^- is smaller than octahedral PF_6^-, it is expected that the probability to replace ligands by counterions is larger for NCS^- than for PF_6^-, due to smaller steric hindrance. Moreover, the finite polarity of NCS^-, in contrast to the nonpolar PF_6^-, also increases its ability to approach the complex ion. A crystal water molecule in $[Fe(phen)_3](NCS)_2.H_2O$ may also assist the exchange reaction due to its polarity. It is known in the field of mechanochemistry that a water molecule tends to increase its polarity under mechanical stress because of the loss of the stability of the substrate (30, 31).

The ligand exchange between phen and NCS^- results in a significant lowering of the symmetry in a complex. The loss of the symmetry, in turn, is related to the decrease in the ligand field strength. Thus, the deformation of the crystals under mechanical stress causes the distortion of coordination bonds. This, in turn, brings about the wider distribution of the energy states. This explains all the observed changes in the magnetic behavior of the complexes in a solid state. Further elucidation of ligand–counterion exchange reactions under mechanical stress is ongoing.

CONCLUSION

The milling of iron(II) complexes with 1,10-phenanthroline gives rise to amorphization, the decrease in the ligand field symmetry, and partial exchange between the species of the ligand and the counterion. These changes are much more pronounced for NCS^- as a counterion than for PF_6^- and result in the increase in $\chi_M T$ in two modes, i.e., a jump at temperatures below 20 K and a subsequent gradual increase. The first mode is attributed to the mechanically induced HS state ($^5T_{2g}$), while the second is thermally induced transition from LS ($^1A_{1g}$) to HS ($^5T_{2g}$) states for the distorted complexes with the widened distribution of the ligand field strength.

ACKNOWLEDGMENTS

This work was supported by a Grant-in-Aid for Scientific Research (No. 09490033) from the Ministry of Education, Science, Sports and Culture in Japan.

REFERENCES

1. T. Isobe, T. Igarashi, M. Konishi, and M. Senna, *Mater. Res. Soc. Symp. Proc.* **536,** 383 (1999).
2. O. Kahn, "Molecular Magnetism," 1st ed., p. 53. VCH, New York, 1993.
3. P. Gütlich, A. Hauser, and H. Spiering, *Angew. Chem., Int. Ed. Engl.* **33,** 2024 (1994).
4. J. E. Huheey, *in* "Inorganic Chemistry: Principles of structure and reactivity" (M. Wasserman and L. Lombardo, Eds.), 2nd ed., p. 332. Harper & Row, New York, 1978.
5. P. Gütlich, "Structure and Bonding," Vol. 44, p. 83. Springer-Verlag, Berlin, 1981.
6. E. C. Constable, G. Baum, E. Bill, R. Dyson, R. van Eldik, D. Fenske, S. Kaderli, D. Morris, A. Neubrand, M. Neuburger, D. R. Smith, K. Wieghardt, M. Zehnder, and A. D. Zuberbühler, *Chem. Eur. J.* **5,** 498 (1999).
7. Y. Sohrin, H. Kokusen, and M. Matsui, *Inorg. Chem.* **34,** 3928 (1995).
8. H. A. Goodwin, *Aust. J. Chem.* **17,** 1366 (1964).
9. G. A. Renovitch and W. A. Baker, Jr., *J. Am. Chem. Soc.* **89,** 6377 (1967).
10. C. N. Field, M.-L. Boillot, and R. Clément, *J. Mater. Chem.* **8,** 283 (1998).
11. M. Nakano, S. Okuno, G.-E. Matsubayashi, W. Mori, and M. Katada, *Mol. Cryst. Liq. Cryst.* **286,** 83 (1996).
12. S. K. Tiwary and S. Vasudevan, *Chem. Phys. Lett.* **277,** 84 (1997).
13. S. K. Tiwary and S. Vasudevan, *Inorg. Chem.* **37,** 5239 (1998).
14. N. Tsuchiya, T. Isobe, M. Senna, N. Yoshioka, and H. Inoue, *Solid State Commun.* **99,** 525 (1996).
15. E. König and K. Madeja, *Inorg. Chem.* **6,** 48 (1967).
16. P. Ganguli, P. Gütlich, and W. Müller, *J. Chem. Soc., Dalton Trans.* 441 (1981).
17. E. Avvakumov, "Mechanical methods for the activation of chemical processes," p. 57. Academy NAUKA, Novosibrisk, 1986.
18. J. H. Takemoto and B. Hutchinson, *Inorg. Nucl. Chem. Lett.* **8,** 769 (1972).
19. K. Nakamoto, "Infrared and Raman Spectra of Inorganic and Coordination Compounds," 4th ed., p. 206. Wiley, New York, 1986.
20. D. M. Adams, G. J. Long, and A. D. Williams, *Inorg. Chem.* **21,** 1049 (1982).
21. J. H. Takemoto and B. Hutchinson, *Inorg. Chem.* **12,** 705 (1973).
22. E. König and K. Madeja, *Spectrochim. Acta A* **23,** 45 (1967).
23. D. A. Thronton and G. M. Watkins, *J. Coord. Chem.* **25,** 299 (1992).
24. B. Hutchinson, J. Takemoto, and K. Nakamoto, *J. Am. Chem. Soc.* **92,** 3335 (1970).
25. Y. Saito, J. Takemoto, B. Hutchinson, and K. Nakamoto, *Inorg. Chem.* **11,** 2003 (1972).

26. Y. Maeda, H. Ohshio, and Y. Takashima, *Bull. Chem. Soc. Jpn.* **53,** 1312 (1980).
27. G. M. Bryant, J. E. Fergusson, and H. K. J. Powell, *Aust. J. Chem.* **24,** 257 (1971).
28. P. Adler, H. Spiering, and P. Gütlich, *Inorg. Chem.* **26,** 3840 (1987).
29. F. Grandjean, G. J. Long, B. B. Hutchinson, L. N. Ohlhausen, P. Neill, and J. D. Halcomb, *Inorg. Chem.* **28,** 4406 (1989).
30. Y. Fujiwara, T. Isobe, M. Senna, and J. Tanaka, *J. Phys. Chem.* **103,** 9842 (1999).
31. Y. Fujiwara, T. Isobe, M. Senna, and J. Tanaka, *Mater. Res. Forum.* **343–346,** 447 (2000).